

# Serial grey-box model of a stratified thermal tank for hierarchical control of a solar plant

Manuel R. Arahál<sup>a,\*</sup>, Cristina M. Cirre<sup>b</sup>, Manuel Berenguel<sup>c</sup>

<sup>a</sup> *Universidad de Sevilla, Dpto. de Ingeniería de Sistemas y Automática, Camino de los Descubrimientos s/n, 41092 Sevilla, Spain*

<sup>b</sup> *Convenio Universidad de Almería-Plataforma Solar de Almería, Ctra. Senés s/n, 04200 Tabernas, Almería, Spain*

<sup>c</sup> *Universidad de Almería, Dpto. Lenguajes y Computación, Ctra. Sacramento s/n, 04120, Almería, Spain*

Received 9 April 2007; received in revised form 11 October 2007; accepted 12 October 2007

Available online 20 November 2007

Communicated by: Associate Editor Halime O. Paksoy

---

## Abstract

The ACUREX collector field together with a thermal storage tank and a power conversion system forms the Small Solar Power Systems plant of the Plataforma Solar de Almería, a facility that has been used for research for the last 25 years. A simulator of the collector field produced by the last author has been available to and used as a test-bed for control strategies. Up to now, however, there is not a model for the whole plant. Such model is needed for hierarchical control schemes also proposed by the authors. In this paper a model of the thermal storage tank is derived using the Simultaneous Perturbation Stochastic Approximation technique to adjust the parameters of a serial grey-box model structure. The benefits of the proposed approach are discussed in the context of the intended use, requiring a model capable of simulating the behavior of the storage tank with low computational load and low error over medium to large horizons. The model is tested against real data in a variety of situations showing its performance in terms of simulation error in the temperature profile and in the usable energy stored in the tank. The results obtained demonstrate the viability of the proposed approach.  
© 2007 Elsevier Ltd. All rights reserved.

*Keywords:* Automatic control; Hierarchical control; Identification; Modelling; Solar energy

---

## 1. Introduction

The Plataforma Solar de Almería (PSA), Spain was built in 1981 as part of the International Energy Agency project entitled Small Solar Power Systems (SSPS). The initial elements of the plant included the ACUREX field, distributed collector system using parabolic troughs to heat oil as in most plants. The processes usually connected to such fields for electricity generation or seawater desalination (Zarza, 1991) are most efficient when operated continuously. To do this they must be provided with a constant supply of hot oil at some pre-specified temperature. This requirement prompted the use of a storage tank as a buffer between

solar collection and the power conversion system (PCS) on early plants such as the SSPS system at the PSA. Whilst these facilities enable the overall plant power output to be maintained during shortfalls, they do not remove the requirement for a fixed quality energy output from the field, in the form of tight outlet temperature control (Meaburn and Hughes, 1996).

Several models of the ACUREX field have been developed mainly for control purposes (Camacho et al., 1997; Camacho et al., 2007). A simulator of the collector field produced by the last author has been available to and used by many researchers (Camacho et al., 1997). The storage tank and PCS however have not received such attention until recently. This is in contrast with the industry trend to increase automation of processes (Prada, 2004). Such trend has caused a need to obtain global models of the plants to be controlled in order to improve final performance,

---

\* Corresponding author. Tel.: +34 954 487 353; fax: +34 954 487 340.  
E-mail address: [arahal@esi.us.es](mailto:arahal@esi.us.es) (M.R. Arahál).

including optimization techniques and hierarchical control strategies.

Hierarchical control consists of decomposing the original task into orderer subtasks, and then handling each sub-task with a specific control (Brdys and Tatjewski, 2005). The structure proposed by the authors can be seen in Fig. 1. It consists of two layers that involve systems with different time scales: the upper layer (slow dynamics) solves an optimization problem as a function of the expected generation and its associate costs. It maximizes the expected profit based on current state of the plant, predicted atmospheric condition, prices and costs and also operating safety constrains. The output of this layer is a set point or reference signal used by the lower layer. This second layer (fast dynamics) includes controllers that ensure set-point tracking. Some previous work regarding hierarchical control of the PSA have been implemented and tested by the authors in Cirre et al. (2004), Berenguel et al. (2005), Cirre et al. (2006), using just a model of the collector field. It is worth remarking that the time scales of the several sub-systems are quite different from one another, being the storage tank the one with slower dynamics and thus the most important for the upper layer of hierarchical control. Following this line of research, a model of the thermal tank is derived here to be later included in order to produce better predictions of the expected profit to be taken into account by the first layer of the hierarchical control structure.

The grey-box approach to model construction (Ljung, 1987) stems from the fact that it is best to take advantage of the a priori knowledge of a system. This knowledge is usually expressed in terms of a set of ordinary or partial differential equations obtained from first principles. For some systems such equations are not completely known and data has to be used to fill-in the gap via an identification procedure. Grey-box models combine a priori knowledge expressed in terms of a phenomenological, or white-box model, with an identification procedure similar to that of black-box models. In most cases grey-box models

have better generalization characteristics than the pure black-box ones and require less amount of data for the identification phase.

Grey-box models have been classified (Thompson and Kramer, 1994) into two categories: (i) serial grey-box (SGB) models that deliver intermediate values of parameters or variables for use in phenomenological models (Van Can et al., 1996), and (ii) models in parallel with a white box model, adjusted to compensate for modelling errors. The results reported in this paper for the storage tank of the SSPS at the PSA are of a SGB model. The identification part uses data obtained at the plant in different operating situations. A simultaneous perturbation stochastic approximation SPSA optimization procedure has been used to adjust the parameters of the model to the observed data. The SPSA algorithm (Spall, 1998) provides an estimation of the gradient of a objective function to be optimized, making it appropriate for high-dimensional optimization problems. An interesting feature is that SPSA can be used in situations where the objective function is contaminated by noise. Also the gradient approximation is deliberately different from the alleged true gradient and this provides a mean to escape from local minima while retaining the desired local convergence property. In the present case the objective function is a measure of the simulation error given by the model.

The paper is organized as follows: Section 2 describes in detail the storage tank within the SSPS at the PSA. The SGB model is introduced in Section 3 along with the SPSA procedure used to adjust its parameters. The benefits of using a grey-box approach are discussed in the context of the intended use of the model in a hierarchical control system. The resulting model is tested against real data in a variety of situations in Section 5 showing its performance in terms of simulation error. The results are discussed with respect to the relevant aspects required by the hierarchical control system. The paper ends with some conclusions.

## 2. Plant description

The distributed collector field consists of 480 east-west aligned single axis tracking collectors with a total aperture mirrors area of 2672 m<sup>2</sup>. The heat transfer fluid used is Santotherm 55 thermal oil, able to withstand temperatures up to 300 °C. The oil resides inside a thermal storage tank, placed near to the solar field. Thermal stratification of the oil in the tank allows storage of energy at different temperatures. The storage tank is connected to the solar field and to the PCS by means of two pipe circuits placed at the top and bottom of the tank (see Fig. 2). The heated oil stored in the tank is used to boil water that is utilized in a steam turbine to drive the PCS.

Normal operation of the plant involves pumping the cold oil from the bottom of the tank to the solar field where it is heated and returned to the tank at the top. From the point of view of control, the manipulated variable is the oil flow rate given by the pump. Changing this flow rate

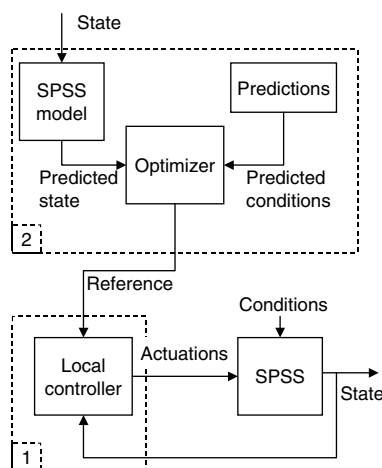


Fig. 1. Diagram of the hierarchical control of the SPSS plant at the PSA.

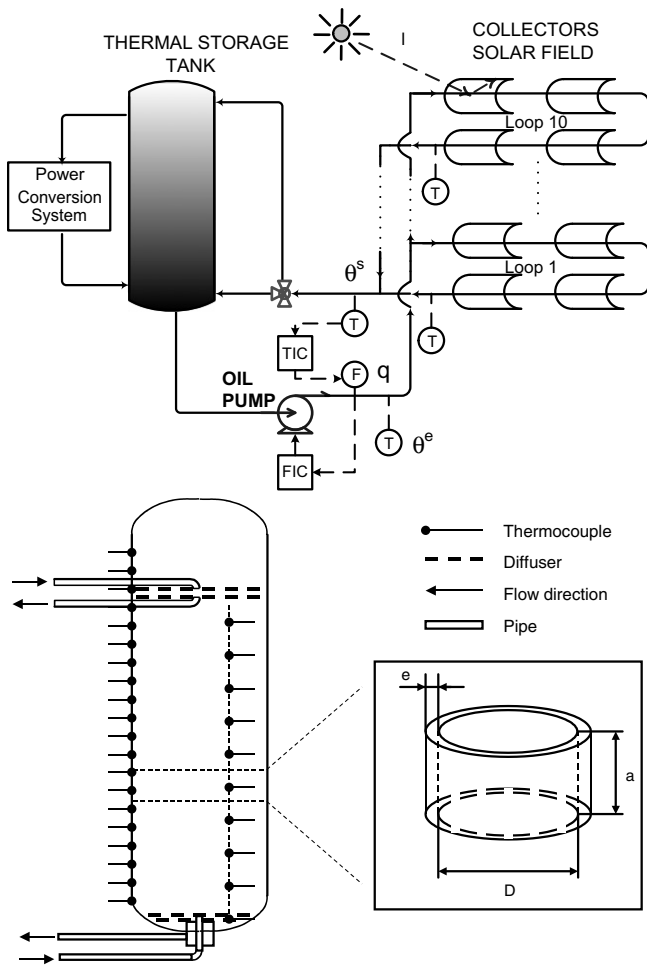


Fig. 2. Top: schematic layout of the SPSS plant at the PSA. Bottom: diagram of the tank showing the location of the thermocouples and pipes. The inset shows a generic discrete control volume used for modelling.

it is possible to control the outlet temperature to some extent. When operating this plant several constraints should be considered in flow rate (between  $2.0$  and  $12.0 \text{ l s}^{-1}$ ), in oil temperature ( $305^\circ\text{C}$ ) and in temperature increments along the pipes ( $70^\circ\text{C}$ ).

The operation of the PCS is activated when there are several layers between  $285^\circ\text{C}$  and  $295^\circ\text{C}$ . In that case, the tank can be considered as loaded and ready to be used. The electricity production can be done in three ways. The first mode of operation is used just when there is not solar radiation to be used, then the hot oil is taken from the tank to the turbine but it does not circulate along the solar field. The second mode of operation is usual when there are large disturbances in solar radiation. The power conversion system is then run using the thermal energy stored inside the tank jointly with solar field, but the oil from the field is sent to the bottom of the tank thanks to a three way valve. This is done in order to avoid temperature fluctuations at the top of the tank. The third mode of operation is used when the levels of solar radiation are good, then the oil from the field is sent to the top of the tank to be used by the PCS.

The lower part of Fig. 2 shows a detailed description of the tank geometric characteristics. Note how the oil entrance and exit contain several diffusers used to avoid disturbances in the oil stratification. Also the position of the thermocouples in the oil and in the wall of the tank is shown in the figure. These thermocouples provide temperature measurements that will be used in the identification part of the modelling procedure.

### 3. Model structure

The model structure for the thermal storage tank corresponds to a discrete-time set of first order equations. This structure has been chosen to achieve the main goals set for the model:

- Long term prediction capabilities that allows it to be used in the upper layer of a hierarchical control strategy.
- Adequate representation of the distributed energy content of the tank. The PCS does not operate in the same conditions for the wide range of temperatures resulting of stratification. For this reason the model must reflect the temperature gradient and its changes during charge or usage periods.
- Low computational load during its use in simulation. In this way the optimization in the upper layer of the hierarchical controller can be run often and deeply enough to provide a quasi-optimum solution under different scenarios.
- Low dependence on the sample time in order to be able to use historical data coming from different experiments.
- Good convergence capabilities in order to diminish the influence of a partially known or noise corrupted initial state.

The basic principles acting on a storage tank are just heat and mass transfer laws. A first principle model seems thus a good choice. However it is a well known fact that some parameters such as heat transfer coefficients among interfaces are difficult to measure. This is specially true for systems whose distributed nature can not be overlooked. This is the case of the storage tank since stratification of temperatures along the vertical direction affects the spatial distribution of the oil parameters. Even in this case a set of partial differential equations adequately adjusted to the particularities of the tank will yield an excellent model. Unfortunately the computational load to run such a model in the many simulations needed for the hierarchical control scheme completely rules out this choice. A common approach for creating models in the situation faced is the so called black box modelling (Ljung, 1987). The black box models are designed entirely from data using no physical or verbal insight whatsoever. The mathematical structure of such models are chosen from families that provide enough flexibility to accommodate most of the informative content of the data. This also means that the model parameters lack significance; they are tuned just to fit the

observed data according to some rule. Grey box models combine the ease of black box models for obtaining parameters from data via identification with a structure provided by any insight that the modeler might have about the system. Traditional grey box approaches assume that the structure of the model is given directly as a parameterized mathematical function partly based on physical principles. In the present case a computer program or algorithm serves as well for the same purpose and has the advantage of being directly the same object later used by the hierarchical controller.

In the remainder of the section the a priori knowledge is presented together with a spatial discretization to produce a simulation algorithm that is in fact the model of the tank. The algorithm contains a set of parameters that will be estimated in the next section using data from the plant.

### 3.1. Spatial discretization

For purposes of modelling the oil and wall of the tank will be divided into sections to form control volumes and control anular sections, respectively. This spatial discretization will follow the particular arrangement of thermocouples along a vertical rod placed inside the tank, yielding ten oil volumes. The thermocouples of the wall are located at different heights and their number is different (twenty instead of ten). To match the temperature measurements on the wall with the temperatures of the discrete anular sections a simple interpolation procedure has been used. The inset in Fig. 2 shows a diagram of the oil volumes and wall anular sections considered. The geometric parameters are the interior diameter  $D$ , the wall thickness  $e$  and the height  $a$  which is the same for all volumes except the lower and upper ones. Other geometrical features such as surfaces can be obtained from the above parameters except in some special cases that will be described below.

### 3.2. Heat transfer models

For each volume a number of models are considered to describe the heat transfer. A simplifying assumption is that conditions (i.e. temperature  $\theta^o$ , density  $d^o$  and specific heat  $c^o$ ) of oil on a given volume are homogeneous. This introduces a source of error in the model since the temperature profile can be very steep causing conditions within one volume to vary appreciably from bottom to top. This is unavoidable since there are no other measurements than those provided by the thermocouples. In the following the different models are introduced:

**Transport.** During operation oil moves along control volumes causing changes in their energy content. The different modes of operation: charge of the tank with hot oil from the field, simultaneous charge and discharge, and discharge with or without recirculation of oil cause different values of the net flow through the tank. A mass flow  $q$  is considered to be positive when it goes from top to bottom which is the normal situation during charge of the tank.

**Conduction.** The energy flow between adjacent oil volumes and between adjacent wall segments due to conduction is modelled in the usual way as a linear function of the temperature increment. The distances among volumes centers are known and depend on the particular disposition of thermocouples. The thermal conductivity  $k^o$  of oil is computed from tables using the average temperature of the volume  $\theta^o$ . For the wall section the thermal conductivity is considered constant.

**Convection.** The convection mechanism is the trickiest in this model. It is difficult to model since it involves effects such as turbulence. The detailed modelling of such phenomenon is absolutely out of the question due to the limitations imposed on the computing load for the final model. The effects produced by convection are however easy to describe: when hot oil enters the bottom of the tank there is a quick mix with the cooler layers above that homogenizes the temperature profile very efficiently. From this observation the energy variation in the volumes due to convection is modelled using: (i) a coefficient that determines the amount of energy that the recirculating flow of hot oil from the collectors yields to the tank and (ii) a set of equations that ensure that this energy is efficiently distributed over the layers above. In this way the simplicity of the model is kept while producing a mechanism that performs well in the simulations as will be shown later.

### 3.3. Simulation algorithm

The simulation algorithm is based in computing the changes in temperature over time for each oil volume ( $\theta_i^o$ ) and wall segment ( $\theta_i^m$ ). The transition from a generic discrete time  $t$  to the next ( $t+1$ ) is governed by the above described heat transfer mechanisms. For each volume  $i = 1, \dots, 10$  the energy change due to transport ( $\Delta E^t$ ), conduction among oil volumes ( $\Delta E^{co}$ ), conduction among wall segments ( $\Delta E^{cm}$ ), convection ( $\Delta E^v$ ), losses from oil to wall ( $\Delta E^w$ ) and from wall to the ambient ( $\Delta E^a$ ) is computed yielding a pair of discrete time equations:

$$\theta_i^o d_i^o c_i^o|_{t+1} = \theta_i^o d_i^o c_i^o|_t + \frac{T_s}{V_i^o} (\Delta E^t + \Delta E^{co} + \Delta E^v - \Delta E^w)|_t \quad (1)$$

$$\theta_i^m d_i^m c_i^m|_{t+1} = \theta_i^m d_i^m c_i^m|_t + \frac{T_s}{V_i^m} (\Delta E^w + \Delta E^{cm} - \Delta E^a)|_t \quad (2)$$

The sampling time  $T_s = 120$  (s) has been selected to provide a good balance between representation of the observed behavior of the temperatures of the volumes and the computational load that it will imply for the simulation. The volume of the discrete elements of oil ( $V_i^o$ ) and metal ( $V_i^m$ ) are computed from geometrical parameters.

## 4. Model adjustment

In the present case the objective function is a measure of the simulation error given by the model. This is so because the intended use of the model is as part of a hierarchical

control scheme providing predictions in large horizons. Besides that some other tests are put on the model such as qualitative concordance with the long term behavior of the plant. By doing so, the goodness of the model for the intended use is thoroughly assessed.

#### 4.1. Model parameters

*Geometric.* The majority of these can be obtained from blue-prints of the plant and measurements made on site. In this category fall all lengths and sections and the location of the thermocouples. There are other such as contact areas that are difficult to measure because they depend on complex geometries arising from pipe intersections and to changing conditions such as the amount of oil in the tank. These parameters will be estimated from data.

*Oil properties.* The producer of the thermal oil provides a table of properties: density, specific heat, conductivity that are function of oil temperature. The data in the tables has been fitted to polynomial functions in order to be used in the model.

*Transfer coefficients.* The heat transfer models for conduction between oil and walls, and between walls and their surroundings are difficult to obtain since they depend on the local conditions of the surfaces. Simplified models affine in the spatial average temperature increment across surfaces are used in this paper. The coefficients for such models will be obtained using data. A special coefficient is the one relating the temperature and flow in the bottom of the tank with the amount of heat transferred to the upper layers during the special operation mode called recirculation. During a recirculation phase the hot oil coming from the collectors enters the tank from the bottom and is sent back to the collectors again. This procedure has two effects: the oil that enters the collectors field gains temperature quickly and the temperature level in the lower part of the tank is also raised causing some homogenization of the temperature profile of the tank.

#### 4.2. Simultaneous perturbation stochastic approximation

The simultaneous perturbation stochastic approximation (SPSA) algorithm is a simultaneous perturbation optimization method that avoids the computation of the gradient. The SPSA technique improves traditional finite difference stochastic approximation (FDSA) methods by using a simultaneous perturbation estimate of the gradient. Only two measurements of the objective function are required at each iteration, regardless of the number of parameters  $n$ , yielding estimates that are comparable FDSA methods for a given number of iterations in terms of accuracy. The SPSA algorithm minimizes an objective function,  $J(\mathbf{x})$  that takes a real-valued vector of search parameters  $\mathbf{x} \in \mathbb{R}$  and returns a scalar measure of goodness of fit. The process begins with an initial guess of  $\mathbf{x}$  that is iteratively adjusted using the direction given by the simultaneous perturbation estimate of the gradient  $\mathbf{g}(\mathbf{x}) = \frac{\partial J}{\partial \mathbf{x}}$

and a gain or step size. The SPSA algorithm consists of the following steps:

- (1) Set  $k = 1$  and apply initial values for  $\mathbf{x}$ .
- (2) Compute the gains as  $a_k = a/(A + k)^\alpha$  and  $c_k = c/k^\gamma$ .
- (3) Compute a random perturbation ( $\delta_k^i$ ) for each component  $i$  of the objective vector using a Bernoulli  $\pm 1$  independent distribution with a probability of 0.5 for each possible outcome. All perturbations are gathered in vector  $\Delta_k \in \mathbb{R}^n$ .
- (4) Evaluate the objective function at two nearby points: The perturbation vector is used to provide  $j_1 = J(\mathbf{x}_k + c_k \Delta_k)$  and  $j_2 = J(\mathbf{x}_k - c_k \Delta_k)$ .
- (5) Approximate the gradient: The simultaneous perturbation approximation of the gradient is computed from  $\hat{\mathbf{g}}(\mathbf{x}_k) = (j_1 - j_2)/(2c_k \Delta_k)$ .
- (6) Update the estimate:  $\mathbf{x}_{k+1} = \mathbf{x}_k - a_k \hat{\mathbf{g}}(\mathbf{x}_k)$ .
- (7) If the termination condition is met finish else go back to step 2.

The algorithm above contains a number of values to be set before its use. These values are called hyper-parameters in order to distinguish them from the parameters of the SGB model and are described below.

- (1) The initial guess is an important issue since it determines the proximity to an acceptable solution. Physical knowledge about the system is of great help in these cases. If no such knowledge is available the initial guess might be in the basin of attraction of a sub-optimal solution. Although the algorithm possess some capabilities to escape local minima there is no guarantee that it will always evade them. A good option then is to run several times the procedure with different starting points.
- (2) Hyper-parameters  $A$ ,  $a$ ,  $\alpha$ ,  $c$  and  $\gamma$  define the sequences that govern the step size at each iteration and the magnitude of the perturbation, respectively. Guidelines for generating these sequences can be found in Spall (1998).
- (3) The termination condition is usually posed in terms of the variation of the current estimate  $\mathbf{x}_{k+1}$  with respect to the previous one  $\mathbf{x}_k$  and can be expressed as  $\|\mathbf{x}_{k+1} - \mathbf{x}_k\| < \epsilon$ . The value of vector  $\epsilon$  is completely problem dependent and has to be handed with care. It is worth noting that in many cases the surface of the objective function is nearly flat close to the optimal solution. Due to this the improvements obtained in  $J$  by subsequent iterations are minimal even for a large number of added iterations. An appropriate choice of  $\epsilon$  prevents the algorithm from performing unnecessary iterations.

In this paper an ad hoc procedure has been used, the value used for  $\epsilon$  is obtained as a fraction  $\beta$  of  $\|\mathbf{x}_1 - \mathbf{x}_k\|$  for  $k > k_{\min}$ , being  $k_{\min}$  a minimum number of iterations that the algorithm is enforced to run. The problem of

obtaining  $\epsilon = \beta \|\mathbf{x}_1 - \mathbf{x}_k\|$  is then reduced to providing  $k_{\min}$  and  $\beta$ . Normally the algorithm reduces the objective function the most in the first iterations and this means that it is little sensitive to the choice of  $k_{\min}$ . Finally the value of  $\beta > 0$  reflects one's confidence in the initial guess. A high value of  $\beta$  means high confidence and little allowance for added iterations beyond  $k_{\min}$ . A small value on the other hand produces a more fine tuning of  $\mathbf{x}$  at the cost of some extra iterations. In spite of the above it is always safe to provide a maximum number of iterations  $k_{\max}$  to avoid excessive long trials. Other termination procedures are discussed in Pluf (1996).

### 4.3. Application of the SPSA

The above algorithm has been applied to the problem of minimizing the mean root squared value of the difference between the true temperature profile and the simulated one. The values of the hyper-parameters used are  $a = 0.16$ ,  $A = 200$ ,  $\alpha = 0.6$ ,  $c = 0.35$ ,  $\gamma = 0.1$ ,  $k_{\min} = 20$ ,  $k_{\max} = 10^3$  and  $\beta = 0.01$ . The parameters used in the objective vector  $\mathbf{x}$  are scaled versions of the unknown parameters of the model. These include:

- Heat transfer coefficient  $k^{ow}$  that models conduction between oil and wall.
- Heat transfer coefficient  $k^{ws}$  that models conduction between wall and surroundings.
- Special coefficient  $k'$  relating the temperature and flow of oil passing through the bottom of the tank in recirculation mode with the amount of heat transferred to the upper strata.
- Special values of contact surfaces between oil and metal for the first  $s_1$  and last discrete element  $s_{10}$  that contain pipe intersections and diffusers.
- Special values of transfer coefficient  $k^{ws}$  that models conduction between wall and surroundings for segments with pipe intersections, namely the first and last.

The scaling of  $\mathbf{x}$  has been done to prevent numerical problems due to the existence in the same vector of components whose magnitude differ in various orders. To produce an adequate scaling suitable initial guesses for each component of  $\mathbf{x}$  have been obtained from common sense and rules of thumb. As a result all components of the objective vector  $\mathbf{x}$  should not be far from unity.

Some measures have been taken during the optimization phase in order to check the validity of results. As is usually done in identification, the available data has been split in a training set (TS) and a validation set (VS). Just data from the TS have been used together with the SPSA procedure to obtain a value of the optimum  $\mathbf{x}^*$ . The data in the VS allows to compare different models corresponding to different values of  $\mathbf{x}^*$  obtained using different hyper-parameters in particular different values of the initial guess  $\mathbf{x}_0$ . In this way the effect of local minima is best avoided (although SPSA has an in-built feature that evades to some extent local minima). At the same time the VS allows to estimate the generalization capabilities of the model. The final assessment of the model however is done with a new set of data not previously used for TS or VS and will be presented in the next section. Fig. 3 shows the evolution of index  $J(\mathbf{x}_k)$  during a typical run of the SPSA algorithm. The values of  $J(\mathbf{x}_k)$  have been obtained for the TS and the VS at each iteration of the algorithm. In the same figure some projections of the evolution of the components of  $\mathbf{x}$  during the optimization are also shown.

### 5. Experimental results and discussion

After the identification phase, data from a new set of experiments are used to assess the generalization capabilities of the model. This validating procedure uses twice as much data than the identification phase. In the discussion that follows different measures of goodness are considered and computed. In all cases the model is used in a simulation

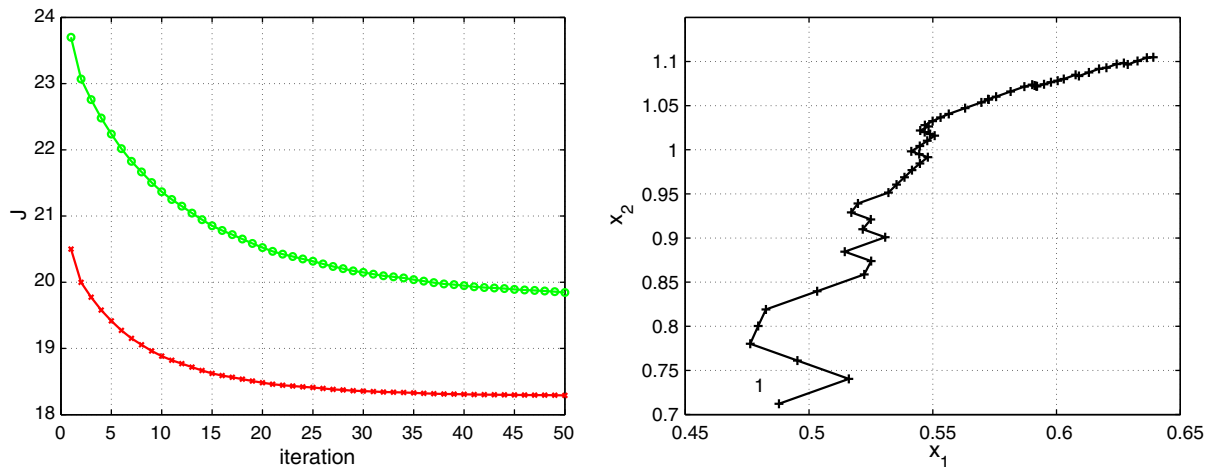


Fig. 3. Left: evolution of index  $J$  during a typical run of the SPSA algorithm in the TS (x marks) and in the VS (circles). Right: projections of the evolution of some of the components of vector  $\mathbf{x}$  during the optimization. The number one at the bottom-left corner marks the projection corresponding to the initial value.

starting at time  $t = t_s$ . The only variables made available to the model are the state at the initial time  $t_s$  and the input variables (flows and temperatures of oil entering the tank from either the collector field or the PCS) at any time  $t \in [t_s, t_f]$ . This means that the model uses its own previous estimation of the state to provide the next one (except in the first step). The initial state is provided as it appears in the data base, which means that it might be noise corrupted or inaccurate in any sense.

### 5.1. Measures of goodness

According to the intended use of the model there are some measures of goodness proposed. In the next paragraphs a mathematical description is given together with a discussion of their relevance. In all cases the measures are obtained using data corresponding to time samples in the interval  $[t_1, t_2]$  where  $t_1 > t_s$  is an appropriately chosen index to take into consideration the effects of initial conditions in the simulation. The final simulation time  $t_2$  is chosen to be similar to simulation horizons used in the hierarchical control scheme where the model is to be employed.

- Temperature profile error. This can be measured by means of the root mean squared simulation error. For each oil volume temperature  $\theta_i^o(t)$  the simulation error is  $e_i(t) = \theta_i^o(t) - \hat{\theta}_i^o(t)$ . This error is accumulated across samples to produce

$$G_i^E = \sqrt{\frac{1}{t_2 - t_1} \sum_{t=t_1+1}^{t_2} e_i(t)^2} \quad i \in \{1, \dots, 10\} \quad (3)$$

- Integral thermal load level. A variable of interest for the hierarchical controller is how much usable energy the tank stores. The usable energy or load level is defined as the energy content at a temperature above a threshold  $U$  that makes it possible for the PCS to work acceptably. The usable energy can be calculated as a function of the number of oil volumes whose temperature exceeds  $U$  and of the temperatures themselves. Let us denote this function as  $I(t) = f(\Theta^o, U)$  where  $\Theta^o \in \mathbb{R}^{10}$  is a vector containing the temperatures of the oil volumes. Function  $f$  is computed as

$$f(\Theta^o, U) := \sum_{i=1}^{10} (0, \theta_i^o - U) \quad (4)$$

For each simulation time the real ( $I(t)$ ) and simulated ( $\hat{I}(t)$ ) load levels are compared and the root mean squared error obtained as

$$G^I(t_1, t_2) = \sqrt{\frac{1}{t_2 - t_1} \sum_{t=t_1+1}^{t_2} (I(t) - \hat{I}(t))^2} \quad (5)$$

The experimental mean and variance of the observed values of the measures of goodness for different experiments give a thorough measure of the performance of the model in simulation.

### 5.2. Validation experiments

A number of new experiments have been performed at the plant to test the validity of the model. The operating conditions for each experiment have been chosen to

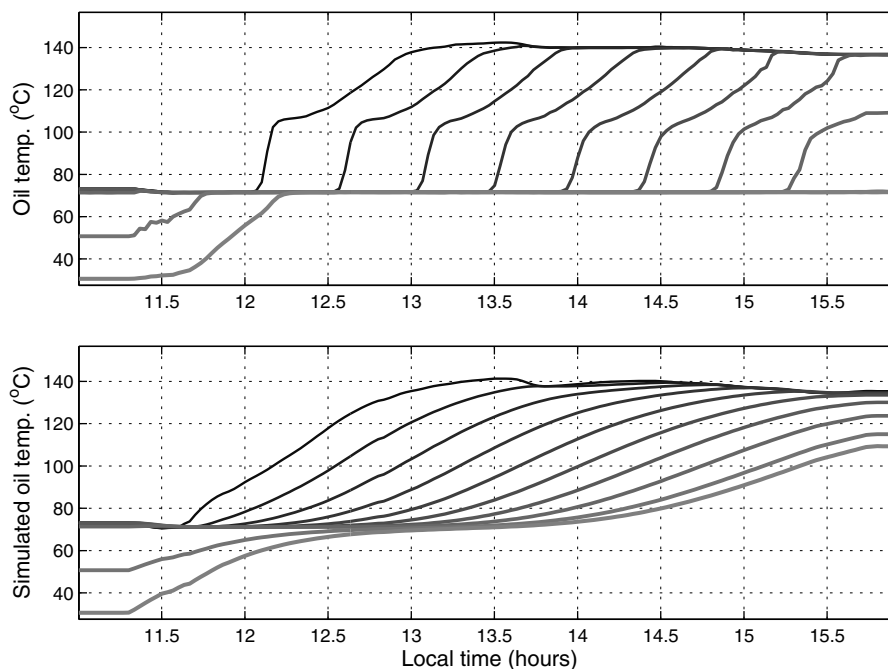


Fig. 4. Evolution of the real and simulated oil temperatures during a validation test. Charging operation at steady high flow rate ( $9 \text{ l s}^{-1}$ ).

represent the various modes of operation of the tank: charge, recirculation, discharge and combinations of these.

In Figs. 4–7 the temporal evolution of variables in some selected validation experiments are shown. In all cases the upper plot correspond to the real evolution of  $\theta_i^o(t)$  and the lower plot to the evolution given by the model during

the simulation ( $\hat{\theta}_i^o(t)$ ). The different curves on each plot correspond to the different components for  $i \in \{1, 2, \dots, 10\}$ , and have a lighter grey tone for higher values of index  $i$ .

Fig. 4 corresponds to a typical charging operation where oil gets heated in the collector field and enters the upper

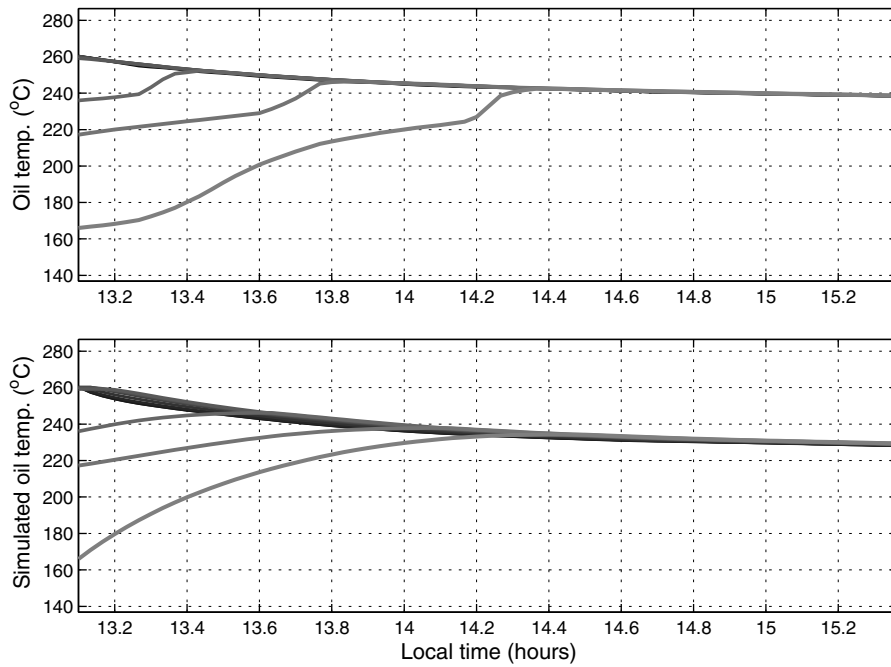


Fig. 5. Evolution of the real and simulated oil temperatures during a validation test. Oil at 200 °C from the collector field is recirculated through the lower part of the tank at medium flow rate ( $5 \text{ l s}^{-1}$ ), producing homogenization.

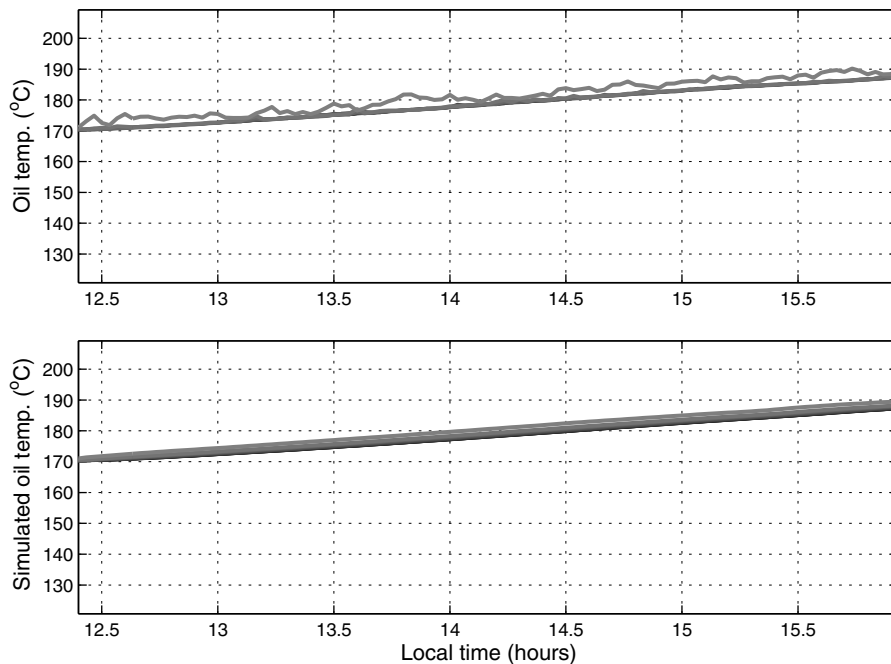


Fig. 6. Evolution of the real and simulated oil temperatures during a validation test. Oil at 240 °C from the collector field is recirculated through the lower part of the tank at medium flow rate ( $5 \text{ l s}^{-1}$ ), producing homogenization and also an increment in the integral load level.

part of the tank (charge mode). It can be seen that due to stratification in the tank the temperatures of the different volumes of oil are significantly different. For a particular volume the temperature raises when the hot oil flows from the top to the bottom due to the circulation produced by the pump that feeds the collector field. Since the thermo-

couples are placed at discrete intervals the temperature changes are very steep. The temperatures given by the model show changes that are smoother due to the simplifying assumptions made. This is not a great problem because the long term trajectories and the integral load level are well captured as will be shown later.

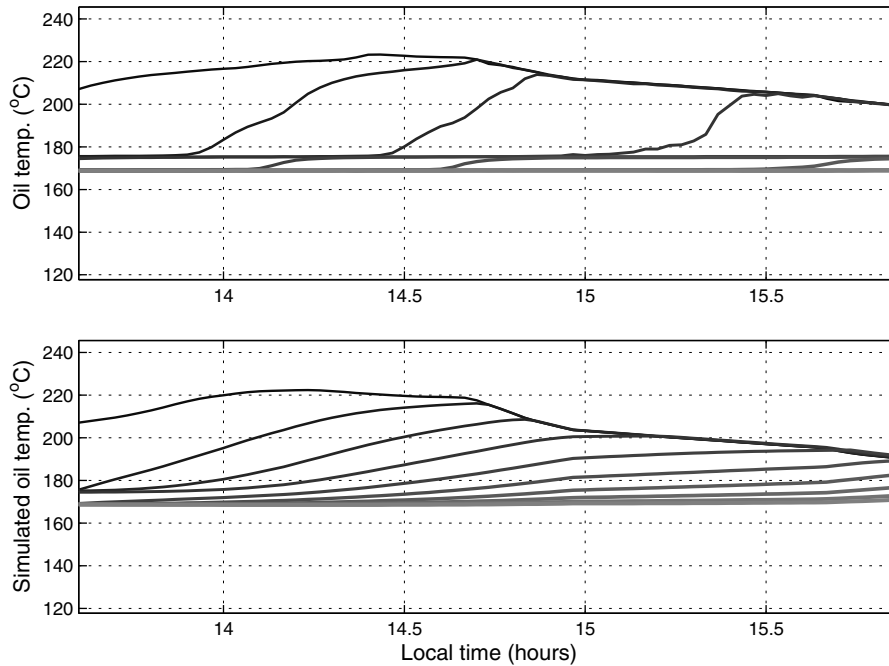


Fig. 7. Evolution of the real and simulated oil temperatures during a validation test. A step change in the flow is performed following a decline in the temperature at the output of the field during automatic control operation as can be seen in Fig. 8.

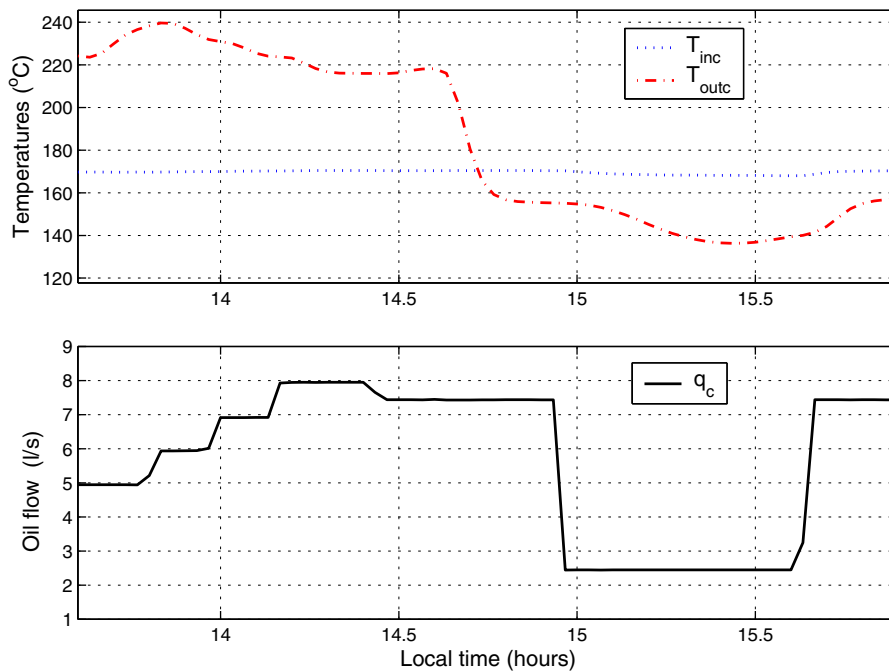


Fig. 8. Evolution of the temperatures at the input and output of the collector field and of the flow rate for the validation test of Fig. 7.

The plots in Fig. 5 are from an experiment in which hot oil coming from the collector field at 200 °C is recirculated through the lower part of the tank, producing a mixing effect that homogenizes the temperature profile and at the same time cooling the upper strata. Similarly in Fig. 6 the recirculation of hot oil at 240 °C produces homogenization and also an increment in the integral load level.

The last graph corresponds to a test where a step change in the flow is performed following a decline in the temperature at the output of the field during automatic control operation. The evolution in the real and simulated oil flow temperatures are given in Fig. 7. The temperature at the input and output of the collector field and the oil flow during this test are shown in Fig. 8. Again some mismatch is observed during the transient phase being the long term behavior correctly modelled (Table 1).

The measures of goodness for the previous and some other experiments are given in Tables 2 and 3. It can be seen that the largest errors occurs in the top layer of the

tank. This is mainly due to the fact that uppermost thermocouple yields sudden and large changes in the measured temperature due to its location close to the oil entrance. The sudden changes are due to the stratification in the tank. This stratification can not be perfectly modelled because only ten discrete volumes are considered by the model. The simplifying assumptions used to derive the equations for each control volume produce a mixing effect within the volume that is observed in the model response. This mixing effect does not take place in the real tank. To alleviate this problem more thermocouples should be added. However this is not necessary because the intended use of the model allows for some mismatch in the temperature transients as long as the long term behavior is correctly captured. It can also be seen that the simulated values of the integral thermal load level are very accurate even in experiments with different types of changes operating at the same time.

## 6. Conclusions

The thermal storage tank of the PSA has been modelled using a serial grey-box approach whose parameters have been obtained from data using the SPSA optimization algorithm. The model is to be used in hierarchical control schemes also proposed by the authors.

The resulting grey-box model produces accurate predictions over sufficiently large simulation horizons with very low computational demand. The tests performed with a new set of real data in a variety of situations show that the generalization capabilities of the model are adequate. In particular it is interesting to note that the simplifying assumptions and limitations arising from the crude spatial discretization have a noticeable effect just in the transient of the temperature profile. The usable energy of the tank is well matched by the model in all tested situations.

Table 1  
Parameters of the models

| Parameter       | Description          | Units             |
|-----------------|----------------------|-------------------|
| $c^{si}$        | Specific heat        | J/(kg K)          |
| $\rho^{si}$     | Density              | kg/m <sup>3</sup> |
| $\Delta E^{sc}$ | Energy change        | J                 |
| $k^{sa}$        | Thermal conductivity | W/m/K             |
| $\theta^{si}$   | Temperature          | K – °C            |
| $q$             | Mass flow rate       | kg/s              |
| $s^i$           | Contact surfaces     | m <sup>2</sup>    |
| $V$             | Volume               | m <sup>3</sup>    |

sa: {ow: oil-wall, ws: wall-surroundings, r: recirculation}.

si: {e: inlet, s: outlet, o: oil, m: walls}.

se: {t: transport, co: conduction among oil volumes, cm: conduction among wall segments, v: convection, w: losses from oil to wall, a: losses from wall to the ambient}.

Table 2  
Measures of goodness in the validation experiments

| Test               | $G_{01}^E$ | $G_{02}^E$ | $G_{03}^E$ | $G_{04}^E$ | $G_{05}^E$ | $G_{06}^E$ | $G_{07}^E$ | $G_{08}^E$ | $G_{09}^E$ | $G_{10}^E$ |
|--------------------|------------|------------|------------|------------|------------|------------|------------|------------|------------|------------|
| 1                  | 37.768     | 19.188     | 4.485      | 4.755      | 4.788      | 5.066      | 5.293      | 5.623      | 5.628      | 6.883      |
| 2                  | 15.100     | 4.048      | 4.300      | 4.404      | 4.367      | 4.639      | 4.838      | 5.133      | 5.080      | 5.785      |
| 3                  | 0.108      | 0.037      | 0.111      | 0.161      | 0.032      | 0.105      | 0.147      | 0.163      | 0.025      | 0.101      |
| 4                  | 1.499      | 13.649     | 22.402     | 27.763     | 18.702     | 10.183     | 4.874      | 2.096      | 0.681      | 0.393      |
| 5                  | 8.444      | 8.716      | 6.872      | 3.871      | 1.785      | 2.000      | 2.549      | 2.950      | 2.987      | 2.811      |
| 6                  | 6.557      | 13.556     | 15.614     | 17.298     | 18.767     | 19.001     | 13.160     | 8.077      | 4.420      | 2.936      |
| 7                  | 5.736      | 7.759      | 9.833      | 11.345     | 12.906     | 14.256     | 15.597     | 17.060     | 19.305     | 16.196     |
| Mean               | 10.745     | 9.565      | 9.088      | 9.942      | 8.764      | 7.893      | 6.637      | 5.872      | 5.447      | 5.015      |
| Standard deviation | 11.927     | 5.981      | 7.071      | 8.974      | 7.330      | 6.359      | 5.207      | 5.155      | 5.993      | 5.124      |

Table 3  
Measures of goodness in the validation experiments,  $\overline{G^E}$  is the mean value across sections of  $G_i^E$  for a given test

| Test                  | 1     | 2     | 3     | 4     | 5     | 6     | 7     |
|-----------------------|-------|-------|-------|-------|-------|-------|-------|
| $\overline{G^E}$ (°C) | 9.948 | 5.769 | 0.099 | 10.22 | 4.298 | 11.93 | 12.99 |
| $G^I$ (%)             | 6.948 | 0.919 | 0.100 | 2.174 | 4.298 | 0.200 | 0.300 |

## Acknowledgement

This work has been financed by project CICYT DPI2007-66718-C04-04 and PNAGI (ECI/2136/2005) at the PSA 2007.

## References

- Berenguel, M., Cirre, C.M., Klempous, R., Maciejewski, H., Nikodem, M., Nikodem, J., Rudas, I., Valenzuela, L., 2005. Hierarchical control of a distributed solar collector field. *Lecture Notes in Computer Science* 3643, 614–620.
- Brdys, M.A., Tatjewski, P., 2005. *Iterative Algorithms for Multilayer Optimizing Control*. Imperial College Press.
- Camacho, E.F., Berenguel, M., Rubio, F.R., 1997. *Advanced Control of Solar Plants*. Springer.
- Camacho, E.F., Rubio, F.R., Berenguel, M., Valenzuela, L., 2007. A survey on control schemes for distributed solar collector fields. part i: Modeling and basic control approaches. *Solar Energy*, web doi: 10.1016/j.solener.2007.01.002.
- Cirre, C.M., Berenguel, M., Valenzuela, L., Klempous, R., 2006. Reference governor optimization and control of a distributed solar collector field. In: *Proceedings of the Euro 2006 Conference, 21st European Conference on Operational Research, Reykiavik, Iceland*.
- Cirre, C.M., Valenzuela, L., Berenguel, M., Camacho, E.F., 2004. Control de plantas solares con generación automática de consignas. *Revista Iberoamericana de Automática e Informática Industrial* 1 (1), 50–56.
- Ljung, L., 1987. *System Identification*. Prentice Hall.
- Meaburn, A., Hughes, F.M., 1996. A simple predictive controller for use on large scale arrays of parabolic trough collectors. *Solar Energy* 56 (6), 583–595.
- Pluf, G.C., 1996. *Optimization of Stochastic Models: The Interface Between Simulation and Optimization*. Kluwer Academic, Boston.
- Prada, C., 2004. El futuro del control de procesos. *Revista Iberoamericana de Automática e Informática Industrial* 1 (1), 5–14.
- Spall, J.C., 1998. Implementation of the simultaneous perturbation algorithm for stochastic optimization. *IEEE Transactions on Aerospace and Electronic Systems* 34 (3), 817–823.
- Thompson, M., Kramer, M., 1994. Modeling chemical processes using prior knowledge and neural networks. *Computers and Chemical Engineering* 40 (8), 1328–1340.
- Van Can, H., Hellinga, C., Luyben, K., Heijnen, J., 1996. Strategy for dynamic process based on neural network in macroscopic balances. *AIChE Journal* 42, 3403–3418.
- Zarza, E., 1991. Solar thermal desalination project. First phase results & second phase description. CIEMAT.